FERMILAB-CONF-14-502-ND

Quasi-Elastic Scattering and Pion Production at MINERνA

M. Betancourt
Fermi National Accelerator Laboratory,
Batavia, Illinois 60510, USA

MINERνA is a neutrino scattering experiment to make precision measurements of cross sections and investigate nuclear effects. A precise understanding of quasi-elastic and charged pion interactions is crucial to neutrino oscillation measurements. We present measurements of the differential cross sections for charged-current quasi-elastic scattering of neutrinos, antineutrinos and charged-current inclusive pion production on a hydrocarbon target. Comparisons of measurements with theoretical models are reported. We find the shape of the quasi-elastic differential cross section for neutrinos and antineutrinos disfavor a simple Relativistic Fermi Gas model and for charged-current pion differential cross section the data is consistent with the GENIE simulation using final state interactions.

1 Introduction

Accurate neutrino cross section measurements and studies of nuclear effects are required for precise measurements of neutrino oscillation parameters, CP-violation in the lepton sector and the orientation of the neutrino mass hierarchy. The charged-current Quasi-Elastic (CCQE) scattering and pion production interactions are very important channels for neutrino oscillation experiments. Experiments such as T2K use CCQE interactions as the main channel for appearance and disappearance measurements [1], while the pion production is one of the most important background in both analyses.

The MINERνA experiment is designed to perform precision measurements of neutrino-nucleus scattering using neutrinos and antineutrinos. We present the first results of differential cross sections of CCQE scattering for neutrinos and antineutrinos, as well as for charged-current pion production.

2 The MINERνA Experiment

The MINERνA experiment uses neutrinos from the Main Injector (NuMI) beam at Fermi National Accelerator Laboratory [2]. The neutrinos are generated by focusing 120 GeV protons from the main injector onto a graphite target. This interaction produces mesons (pions and kaons), which are focused by two magnetic focusing horns located downstream of the target. The mesons decay and produce neutrinos. Changing the horn current polarity produces either a neutrino or an antineutrino beam.

The MINERνA detector is comprised of 120 hexagonal modules perpendicular to the z-axis, which is tilted upwards by 58 mrad with respect to the beamline. MINERνA is segmented transversely into: the inner detector, with planes of solid scintillator strips mixed with nuclear targets; a region of pure scintillator strips; downstream electromagnetic calorimeter and hadronic calorimeters; and an outer detector composed of a frame of steel with embedded scintillator,

Operated by Fermi Research Alliance, LLC under Contract No. De-AC02-07CH11359 with the United States Department of Energy.

which also serves as the supporting structure. The scintillator strips in adjacent planes are offset by 60° from each other, which enables a three-dimensional track reconstruction [3]. The MINOS near detector is situated two meters downstream of the MINERνA detector and serves as a magnetized muon spectrometer [4].

3 Charged Current Quasi-Elastic Scattering

We have studied the CCQE scattering for neutrinos and antineutrinos using muon kinematics and the quasi-elastic assumption. The selection uses the following criteria: 1)The vertex interaction is required to be in the tracker region (5.8 tons), 2) The muons are matched to MINOS tracks, where the momentum and charge is analyzed (μ^+ for antineutrino and μ^- for neutrino). Since the region near the vertex is not well modeled by the simulations, we exclude a region of 30 cm for neutrinos (ν) and 10 cm for antineutrinos ($\bar{\nu}$) around the vertex, to avoid dependence on the modeling of the event vertex region. In addition, to enhance the quasi-elastic signal the analysis uses a selection of the non-vertex energy as a function of the Q^2, which is reconstructed using the quasi-elastic assumption.

The reconstructed neutrino energy and four momentum transfer Q^2 is calculated by assuming the two-body CCQE kinematics:

$$E_{QE} = \frac{m_n^2 - (m_p - E_b)^2 - m_\mu^2 + 2(m_p - E_b)E_\mu}{2(m_p - E_b - E_\mu + p_\mu \cos\theta_\mu)}, \quad (1)$$

$$Q^2 = m_\mu^2 + 2E_{QE}(E_\mu - p_\mu \cos\theta_\mu) \quad (2)$$

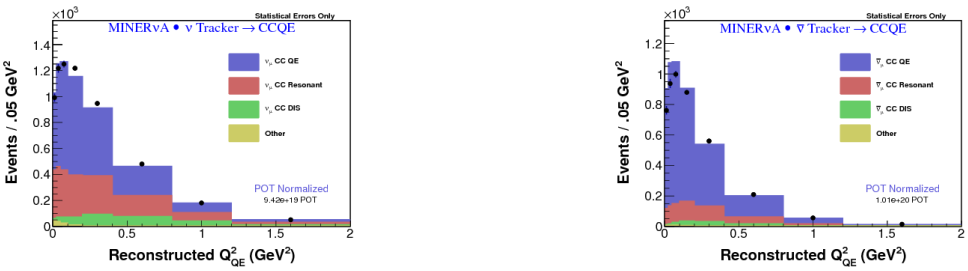

Figure 1 – Reconstructed neutrino energy and Q^2 for neutrinos (left), Reconstructed neutrino energy and Q^2 for antineutrinos (right).

Figure 1 shows the reconstructed four momentum transfer (Q^2). The left panel shows event distribution for neutrinos as a function of Q^2 and the right distribution is for antineutrinos. The distributions show the selected events in data and simulation, the signal is represented by the blue curve (CCQE), the backgrounds are the red, green and yellow curves (CC Resonant, CC DIS and others). The neutrino selection has 47% efficiency and 49% purity and the antineutrino has 54% efficiency and 77% purity. The main background is from resonance production, where the pion from the resonance interaction has been absorbed. A total of 29,620 data events are selected for neutrino and 16,467 for antineutrinos. The data of this analysis come from 9.42×10^{19} protons on target for neutrinos and 1.01×10^{20} protons on target for antineutrinos.

We calculate the differential cross section using the experimental definition $(\frac{\partial\sigma}{\partial Q^2_{QE}})_i = \frac{\sum_j U_{ij}(N_{data,j} - N_{bg,j})}{T\phi\Delta Q^2_{QE}\epsilon_i}$, where U_{ij} is the unfolding matrix to account for the resolution of reconstructed events, $N_{data,j}$ is the number of events in data, $N_{bg,j}$ is the predicted number of background events, T is the number of target nucleons, ϵ_i is the efficiency for i^{th} bin, ϕ is the integrated neutrino flux over the neutrino energy range of 0-10GeV, and ΔQ^2_{QE} is the width of bin i. Figure 2 shows comparisons of the measured differential cross section with respect to Q^2_{QE} and different theoretical models. We use the GENIE and NuWro simulations[5], where

GENIE uses the Relativistic Fermi Gas model (RFG) with an axial mass of $M_A = 0.99GeV/c^2$ and NuWro uses RFG model and different M_A values. In addition, NuWro includes the Spectral Function model (SF), which is a more realistic model of the nucleon momentum, and a transverse enhancement model (TEM) tuned to electron-nucleon scattering data to account for correlated nucleon target[6].

Figure 2 – Differential cross section compared with GENIE and NuWro simulations for the neutrinos analysis(left), differential cross section compared with GENIE and NuWro simulations for the antineutrinos (right).

Figure 3 – Ratio of the measured differential cross section to GENIE and NuWro simulations for neutrinos (left), Ratio of the measured differential cross section to GENIE and NuWro simulations for antineutrinos (right).

Ratio of the measured neutrino and antineutrino $d\sigma/dQ^2$ in Q^2 shape and NuWro predictions to GENIE are shown in figure 3. The data is consistent with the transverse enhancement model (TEM) with $M_A = 0.99GeV/c^2$ [7].

4 Neutrino Pion Production

The selection criteria for this analysis requires a muon and a pion in the final state. The event selection uses, a) A primary vertex within the scintillator tracker, b) A muon track matched to a MINOS track, c) Identification of the pion performed via a particle ID, which uses the energy lost, dE/dx, to separate pions from protons. In addition, the analysis requires a selection in the hadronic invariant mass ($W_{exp} < 1.4GeV$) and a reconstructed neutrino energy less than 10GeV, where the reconstructed energy and hadronic invariant mass are reconstructed using $W^2_{exp} = -Q^2 + m_n^2 + 2m_nE_H$ and $E_\nu = E_\mu + E_H$. The events with hadronic invariant mass $W_{exp} > 1.4GeV$ are removed from the analysis. The full set of analysis selection yield 3474 event candidates with one-pion.

The calculated cross section is shown in figure 4; the left distribution shows the ν_μ charged current $\pi^\pm$ production differential cross section with respect to the $\pi^\pm$ kinetic energy and the right figure shows the differential cross section with respect to the $\pi^\pm$ angle with respect to the beam. The distributions are compared to the GENIE prediction with Final State Interactions (FSI) and without final state interactions (no FSI). Previous measurements from the MiniBooNE experiment showed data to be consistent with a model without final state interactions[8]. The MINERνA charged pion data favor GENIE with FSI included.

We compare the measured differential cross section with different models, using different event generators (GENIE, NuWro and Neut)[5], as well as a theoretical calculation from Athar

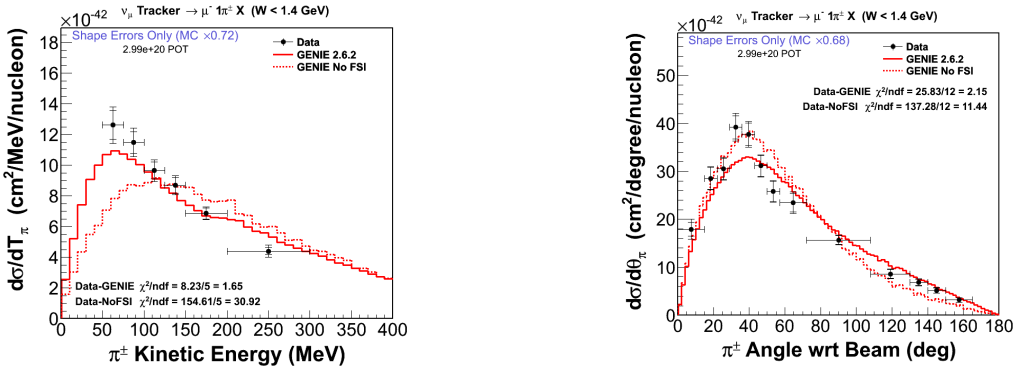

Figure 4 – Charged current $\pi^{\pm}$ production differential cross section with respect to kinetic energy (left), and charged current $\pi^{\pm}$ differential cross section with respect to the angle with respect to the beam.

[9]. Figure 5 shows the measured differential cross sections compared to the different models. We find good shape agreement between data and the different event generators. For the Athar calculation, which contains an incomplete FSI model, the shape of the data does not agree.

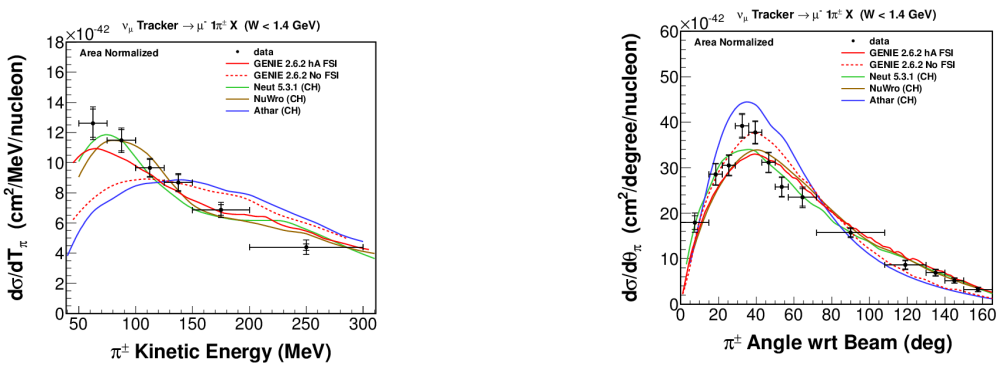

Figure 5 – Comparisons of the one-pion measurements to various models. Charged current $\pi^{\pm}$ production differential cross section with respect to kinetic energy (left), and charged current $\pi^{\pm}$ differential cross section with respect to angle(right).

Conclusions

The first ν_μ and $\bar{\nu}_\mu$ CCQE differential cross sections and neutrino charged-current pion production differential cross section measurements from the MINERνA experiment are reported. The shape of the measured differential cross sections for neutrinos and antineutrinos, $d\sigma/dQ^2$, disfavor a simple Relativistic Fermi Gas model and agree with a transverse enhancement model with $M_A = 0.99 GeV/c^2$. For the charged-current pion production differential cross section measurements $d\sigma/dT_\pi$ and $d\sigma/d\theta_\pi$, the data prefer the GENIE model with final state interactions. The data are also consistent in shape with the NuWro and NEUT event generators with final sate interactions.

Further analyses from the MINERνA experiment are underway to constrain different cross sections, such as $\nu_\mu, \bar{\nu}_\mu$ coherent pion production, charged-current π^0 production, ν_μ charged-current quasi-elastic proton kinematics, ν_e charged-current quasi-elastic and kaon production. All of these analysis are important for neutrino oscillations measurements.

References

1. K. Abe *et al.* [T2K Collaboration], Phys. Rev. Lett. **107**, 041801 (2011); Phys. Rev. Lett. **112**, 068103 (2013).
2. K. Anderson, B. Bernstein, D. Boehnlein, K. R. Bourkland, S. Childress, N. Grossman, J. Hylen and C. James *et al.*, FERMILAB-DESIGN-1998-01.
3. L. Aliaga et al., Nucl. Instrum. Meth. **A743**, 130 (2014).
4. D. G. Michael *et al.*, Nucl. Instrum. Meth., **A596**, 190 (2008).
5. C. Andreopoulos, A. Bell, D. Bhattacharya, F. Cavanna, J. Dobson, S. Dytman, H. Gallagher and P. Guzowski *et al.*, Nucl. Instrum. Meth. A **614** 87 (2010). T. Golan, C. Juszczak, and J. Sobczyk, Phys. Rev. C **85** (2012). R. Smith and E. Moniz, Nucl. Phys. B **43**, 605 (1972).
6. O. Benhar, A. Fabrocini, S. Fantoni, and I. Sick, Nucl.Phys. A **579**, 493 (1994). A. Bodek, H. Budd, and M. Christy, Eur.Phys.J. C**71**, 1726 (2011).
7. G. A. Fiorentini *et al.*, Phys. Rev. Lett. **111**, 022502 (2013). L. Fields *et al.*, Phys. Rev. Lett. **111**, 022501 (2013).
8. A. A. Aguilar-Arevalo, *et al.*, Phys. Rev. D **83**, 052007 (2011).
9. Y. Hayato NEUT, Acta Phys. Pol **40** 2477 (2009). M. S. Athar, S Chauhan and S. K. Singh Eur. Phys. J., **43** (2010).